Dipolar plasma source modeling: a first approach

Stéphane Béchu, Tran Than Vinh, A. Lacoste, A. Bès, M. Rayar, J. Pelletier

Dipolar Plasma Source Modeling: a First Approach

Stéphane Bechu*, Tran Than Vinh, Ana Lacoste, Alexandre Bès, Marius Rayar, Jacques Pelletier

Laboratoire de Physique Subatomique et de Cosmologie
Centre de Recherche Plasma-Matériaux-Nanostructures
Université J. Fourier Grenoble 1, CNRS/IN2P3/ST2I, INP-Grenoble

*Corresponding author: 53 rue de Martyrs, 38026 Grenoble Cedex, France, stephane.bechu@ujf-grenoble.fr

Abstract: The scaling up of conventional plasmas presents limitations in terms of plasma density, limited to the critical density, and of uniformity, due to the difficulty of achieving constant amplitude standing wave patterns along linear microwave applicators in the meter range. An alternative solution lies in the concept of distribution from one- to two-dimensional networks of elementary plasma. Each elementary plasma source consists in a permanent magnet on which microwaves are applied via an independent coaxial line [1]. The plasma is produced by the electrons accelerated at ECR (Electron Cyclotron Resonance) and trapped in the dipolar magnetic field. Large-size uniform plasmas can be obtained by assembling as many such elementary plasma sources as necessary, without any physical or technical limitations [2]. Simulation of the plasma produced by a dipolar source requires a global, self consistent, modeling of its functioning. In order to obtain results to lead a first optimization of the dipolar source, magnetostatics, microwave propagation and fast electrons trajectories (Particles in Cell (PIC) and Monte-Carlo hybrid method [3]) have been performed with Comsol Multiphysics and MatLab.

Keywords: magnetostatics, microwave propagation (2.45 GHz), dipolar plasma, electron trajectories, PIC/Monte-Carlo hybrid method.

1. Introduction

To overcome the difficulty of producing large area plasma of high density (above 10^{12} electrons/cm^3), dipolar source has been designed. Even though a single source is far from producing homogeneous plasma, organized into a one or two-dimensional network, the produced plasma becomes largely homogeneous even at its limits. These elementary plasma sources can be assembled in different ways, e.g. networks of elementary plasma sources with alternate or identical magnetic polarities, rectangular or hexagonal networks, or other combinations [4,5].
An elementary plasma source consist of two main parts, i.e. a permanent magnet with an azimutal symmetry around its magnetization axis, and a microwave applicator constituted by a coaxial line, parallel to the magnetization vector, and open on the rear pole of the magnet. The magnet is completely encapsulated and water-cooled. The microwave power is transmitted without loss to the ECR coupling region around the magnet with the help of the coaxial line.
At the microwave frequency of f_0 = 2.45 GHz, the magnetic field intensity B_0 required for the ECR condition (Eq. 1) is 875 G (1 Gauss = 10^{-4} Tesla).

$$B_0 = 2\,\pi \left(\frac{m_e}{e} \right) f_0 \qquad (1)$$

In this equation, f_0 is the microwave frequency, m_e and -e, the mass and electric charge of the electron, respectively.

For this magnetic field intensity (B_0) electrons rotating at an angular frequency ω_{ce} around B_0 field lines which is the same as a right-hand circularly polarized electric field component. Hence, these electrons are submitted to a constant electric field while they remain in the ECR coupling region, i.e. on a magnetic field line crossing a magnetic intensity of 875 G. Hence, electrons gain energy from the microwave intake power. Such a resonant coupling mechanism can produce very hot electrons (named primary or fast electrons) [6]. Electrons are ejected from ECR coupling area by collision, elastic or inelastic, with neutrals or other plasma species or even when colliding with a wall. An optimized coupling implies a low pressure functioning, in the mTorr range, and a

well design magnetic field to maintain electrons in the ECR zone.
For dipolar source, the permanent magnet used is a cylindrical samarium-cobalt magnet 10 mm or even 30 mm long, 20 mm of outer diameter and 4 mm of inner diameter. It produces 3D trapping zone around the magnet, magnetic field lines converge at each pole. Mirror spots for electron trajectories are created, by the combination of magnetic field gradients and magnetic field lines curvature near the poles.

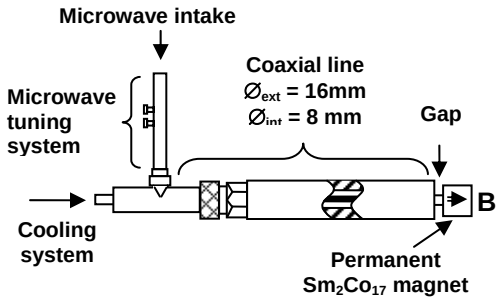

Figure 1. Sketch of the dipolar microwave (2.45 GHz) plasma source. A source consists of a tuning system, a coaxial line (partially under vacuum) and a cooled permanent magnet with an axial **B** field.

High frequency (HF) electric field E(t) resulting from microwaves propagation in the dipolar source and in the plasma chamber is far more difficult to calculate than static magnetic field. The latter is not modified by microwaves or by the created plasma. All materials are not ferro-magnetic; the magnetic field around the magnet is not modified and remains the same as if the magnet lies only in vacuum. Microwave propagation depends on relative permittivity and electric conductivity; these values are modified by the existing plasma (see Equ. 2 and 3).

$$\varepsilon_r = 1 - \frac{\omega_{pe}^2}{\omega(\omega - i\nu)} \qquad (2)$$

$$\sigma_r = \frac{n_e e^2}{m_e(\nu + i\omega)} \qquad (3)$$

Microwave propagation, in plasma medium, needs complex "self consistent schem" for being modeled. This kind of model uses Poisson solvers and particles diffusion codes to take into account the modification of permittivity and conductivity.
Such a complex model is beyond the reach of our calculations. To circumvent this difficulty we have used experimental Langmuir probe measurements to obtain electronic density, n_e, and temperature, T_e around the dipolar source. With these data, we obtained values of ε_r and σ_r in the vicinity of the source. Microwaves propagation calculations with plasma, presented below, uses this method to avoid complex iterative scheme.
Plasma is sustained by electrons of energy above 15.76 eV for argon, via inelastic collisions with neutral. This reaction produces a slower electron and one ion. ECR coupling gives a very efficient way to increase electron energy. Trajectories of such particles are very important to localize plasma creation area. As ECR coupling phenomenon has been modeled only for ideal case [3], infinite length magnet, particles trajectories calculated do not include energy gain for electron. Electrons are launched at arbitraries locations at random speed (centered on 20 eV). Comparison with optical emission spectroscopy measurements (OES) of ion and neutral emission lines was performed. This emission line indicates the localization of fast electrons. Hence, when variations of this emission line are observed, densities of primary electrons are monitored.

Section 2 deals with magnetostatics of the cylindrical Sm_2Co_{17} magnet without and with a iron auxiliary part. The model takes advantage of the rotational symmetry of the problem, only a 2D modeling is performed.
Microwave propagation modeling, in vacuum and in plasma medium, is presented in section 3. A 2D modeling has been also performed.
Fast electrons trajectories are calculated and presented in section 4.
Eventually, in section 5, experimental results obtained from OES of atomic and ionic lines intensity are presented and compared with calculations.
A summary of the obtained calculations and results is made in section 6 and remaining work is briefly exposed.

2. Magnetostatics

As presented in the above section, a permanent magnet, made of Sm_2Co_{17}, is set at the end of the coaxial line. For positioning accurately the 875 G magnetic line, the non-linearity of iron, when used, has been taken into account. For this purpose in our 2D model, the variation of the relative permeability μ_r has been used as follow: $\mu_r = f(B)$. It is a consequence of the definition of $H = f(B, \mu_r)$ used by the solver.

2.1 Model definition
Equations to be resolved are:

$$\nabla \times \mathbf{H} = \mathbf{J} \quad (5)$$

$$\nabla \cdot \mathbf{B} = \mathbf{0} \quad (6)$$

$$\mathbf{B} = \mu \mathbf{H} \quad (7)$$

In our case, **J**, the current density is null. Hence, it is possible to model the permanent magnet using a scalar magnetic potential formulation:

$$\mathrm{H} = -\nabla \mathrm{V_m} \quad (8)$$

2.2 Sub domains settings and boundary conditions
In vacuum, magnetic permeability is given by: $\mu_0 = 4\pi \times 10^{-7}$ H.m^{-1}. In the magnet, the relative permeability is isotrope and issued by the magnet manufacturer (XULONG Magnetics manufactury Co.,Ltd [7]).
For this purpose, the COMSOL multiphysics magnetostatic module, has been used. While PML are not suitable for 2D-axisymetric modeling, a large area around the magnet is defined (175 mm in radius and 350 mm in height). On this domain, 230 000 degrees of freedom was defined.

In the magnet, intensity of magnetic field is defined by:

$$\mathrm{B} = \mu_o \mu_r \mathrm{H} + \mathrm{B_r} \quad (8)$$

$B_r = 1.05$ T for Sm_2Co_{17} magnet.
In iron and air the following equation is used:

$$\mathrm{B} = \mu_o \mu_r \mathrm{H} \quad (9)$$

Boundary conditions are: a magnetic field of very low intensity (10^{-6} G) at the edges of the domain. Intensity of **B** has been measured at 85 mm of the magnet surface in its mid-plan and shows intensity below 20 G. It indicates that a very low B field intensity at boundaries can be settled.

2.3 Results
In Figs. 3 and 4, the line of magnetic field intensity corresponding to ECR coupling (875 G) is indicated by a bold line, the field lines converge at the poles and join the two opposite poles of the magnetic dipole constituted by the magnet.
Comparison between the two figures indicates that existence of an auxiliary iron part behind the magnet does not induce a major modification of magnetic field lines shape. Figure 4 shows that 4 mm thick of iron has shifted the magnet itself and the 875 G line inside the gap. Without this supplementary part, this line crosses over the external conductor of the dipolar source.

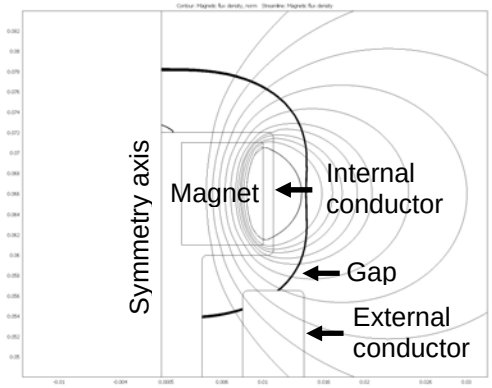

Figure 3. Magnetic field lines, thin lines and line of constant intensity (875 G) in bold type for a magnet of 10 mm height and 20 mm in diameter.

On advantage of shifting the magnetic field line inside the gap instead of intercepting the exterior conductor is the possibility of heating much more electrons by ECR coupling inside the gap where microwave power is delivered.

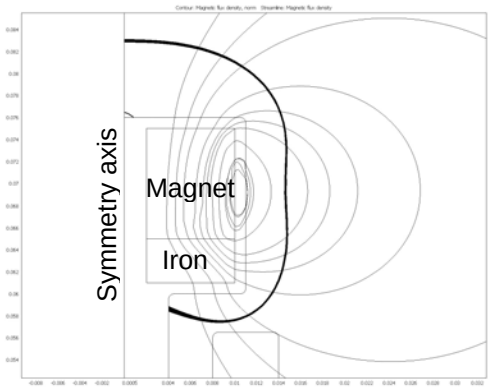

Figure 4. Magnetic field lines, thin lines and line of constant intensity (875 G) in bold line for a magnet of 10 mm height and 20 mm in diameter. An additional part, 4 mm thick of ARMCO iron, is placed at the magnet bottom.

3. Microwave propagation

To achieve ECR coupling mechanism, both static magnetic (presented above) and electromagnetic fields are necessary. Hence, wave propagation modeling inside and outside of the dipolar source is fundamental.

3.1 Model definition

In the main part of the dipolar source, microwave propagates in a coaxial line. The electromagnetic field is transverse electromagnetic (TEM) with a discrepancy in 1/r (r is the radial location). At the end of the coaxial line, where the magnet is located, propagation is modified and is no longer TEM, wave propagates inside the metallic plasma chamber which acts as a resonant cavity.

3.2 Sub domains and boundary settings

Our plasma diffusion chamber has 350 mm in height and 175 mm in radius. In order to have a more accurate definition of the electric field around the dipolar source, a second area has to be defined with interior boundary (for the model) and a refined mesh. For boundary conditions, we have used perfect metallic conductor, as walls are made of aluminum, hence: $\mathrm{n} \times \mathrm{E} = 0$.

3.3 Results

Obtained results show an existing electric field inside the plasma chamber far away from the dipolar source (where microwave power is delivered). Figure. 5 presents these variations (log(norm(E(t))) obtained from modeling.

Hence, before the plasma ignition it appears that the plasma chamber acts as a microwave cavity.

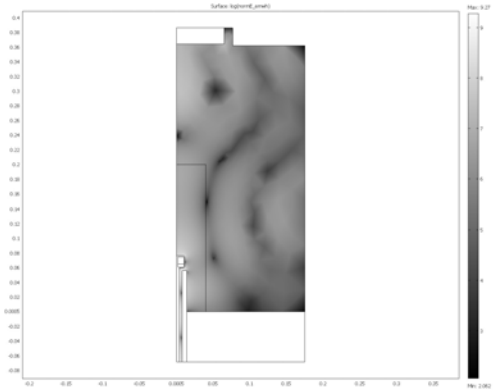

Figure 5. Variations, in vacuum, of log(norm(E)) inside the plasma chamber. Dipolar source is located at the bottom and the symmetry axis is on the left.

Figures 6 gives a close sight of electrical field (iso-values of norm(E(t)) inside the gap and around the magnet. It appears that electric field is more intense inside the gap or at the dipolar source top than in the mid-plan of the magnet.

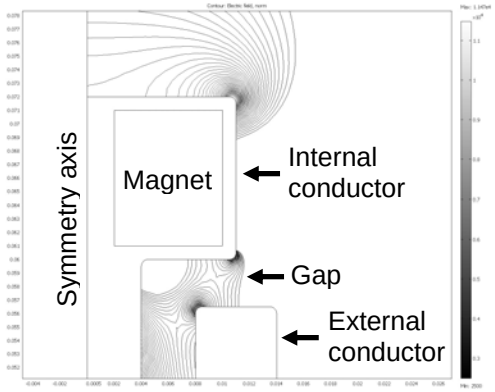

Figure 6. Close view of norm(E) (iso-values) around the dipolar source.

Figure 7 shows experimental data and data used to calculate relative permittivity and electric conductivity around the source with equations 2 and 3. We have divided the area around the dipolar source into 6 arbitrary zones, 5 with an elliptical shape and a last one to fill totally the plasma chamber. In these zones, the plasma is

considered as an isotrope medium of constant parameters (density, temperature, permittivity, conductivity).

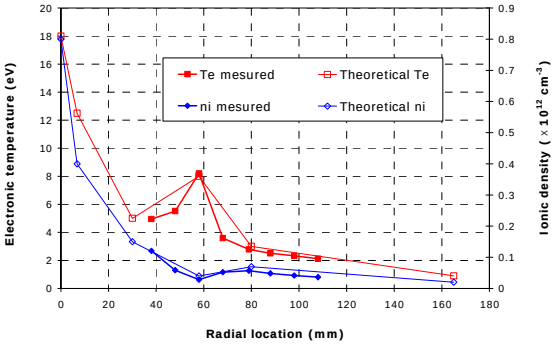

Figure 7. Radial variations (from the magnet's surface) of plasma density (n_i) and electron temperature (T_e) in the mid-plan of the magnet. Experimental data are in filled spots and data used in the model are represented in unfilled spots.

In comparison with microwave propagation in vacuum, the plasma limits the expansion of the alternative electric field far away from the source. The plasma chamber no longer acts as a cavity. Microwave power is largely absorbed in front of the gap.

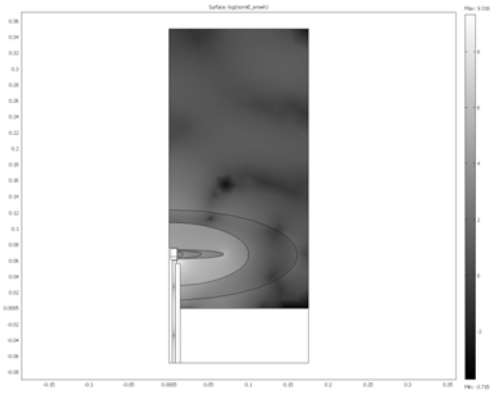

Figure 8. Variations of log(norm(E)) inside the plasma chamber, in vacuum (2.45 GHz). Dipolar source is located at the bottom and the symmetry axis is on the left. Five elliptical shape areas are arbitrary defined around the dipolar source.

A close view of the magnet area, Figure 9, shows a high intensity of the HF field in the gap region. Electric field is no longer present at the top of the source (see Figure 6).

Knowing these results, ones may think as HF field is higher in the gap edge than elsewhere, ECR coupling mechanism takes place in this region. Simple naked eyes observations do not validate this possibility; only glowing rings are observed in the equatorial plan of the magnet.

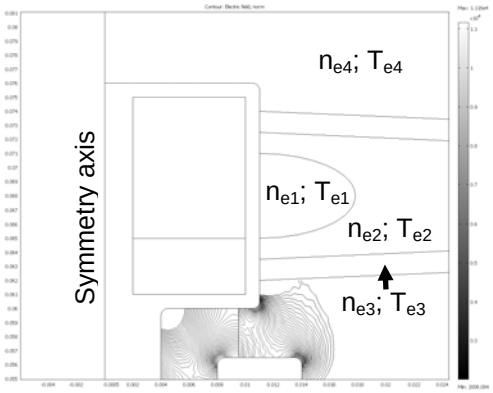

Figure 9. Close view of norm(E) (iso-values) around the dipolar source with plasmas zones. Plasma parameters density and temperature (respectively n_e and T_e) are constant in each zone.

4. Fast electrons trajectories

Trajectories of fast electrons in a multi-polar magnetic field have been studied analytically for infinite length magnets [8]. For finite length magnet, there is no simple analytic equation to describe the magnetic field produced. Hence, a PIC scheme and interpolations between grid nodes must be performed to follow electrons trajectories.

Equations of movements are:

$$\frac{d\mathbf{v}}{dt} = -\frac{e}{m_e}(\mathbf{E} + \mathbf{v}\times\mathbf{B}) \qquad (10)$$

$$\frac{d\mathbf{r}}{dt} = \mathbf{v} \qquad (11)$$

Calculations performed with Matlab, using a leap-frog scheme and a Monte-Carlo, show oscillating trajectories between mirror poles. Monte-Carlo scheme has been used to take into account collisions with neutral. These trajectories are presented on Figure 10.

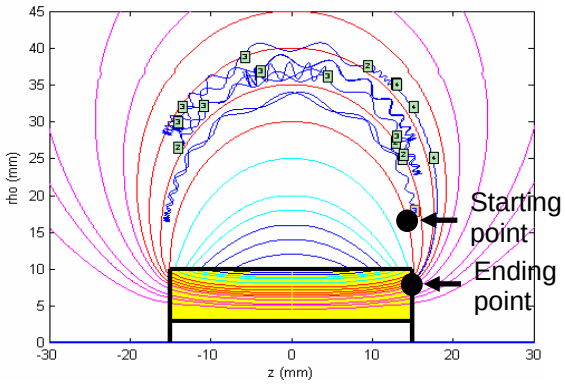

Figure 10. Electron trajectories around a cylindrical magnet of 30 mm in length and 20 mm in diameter. Electron energy is 20 eV distributed randomly over the three components (v_x, v_y and v_z).

These results indicate that electrons spend most of the time in the mid plan of the magnet. At each pole, even if the axial speed component no longer exists, electrons are rapidly reflected toward the opposite pole. Another important feature of these locations (mirrors spots) is the very important magnetic field curvature and gradient.

5. Experimental results

In order to verify the validity of electrons trajectories calculations, OES measurements have been performed along the magnet axis in argon plasma at two different pressures (1 and 2 mTorr).
Variations of atomic to ionic emission lines intensity ratio, respectively 7504 Å and 4609 Å, have been recorded. With such a measurement, even if the plasma thickness varies from one position to another the ratio of emission lines takes it into account. Hence, this measurement indicates relative variations of ions excitations by inelastic collision with fast electrons. The threshold of this excitation is 30 eV. Hence, it is an accurate indicator for fast electrons density mapping.

Figure 11 presents obtained results from OES at two different pressures. Intensity ration is obviously higher in the mid plan of the magnet than is the gap area. It indicates that fast electrons density is higher in the middle of the magnet than where microwaves are distributed, the gap. These results are in good accordance with numerical results which indicate that electron can be more efficiently heated in the mid plan of the magnet than in the gap area.

6. Conclusions

Magnetostatics calculations showed the weak influence of a iron supplementary part placed below the magnet. The physical shift of the magnet, of the iron thickness, sets the 875 G line inside the gap where the microwave power is delivered.

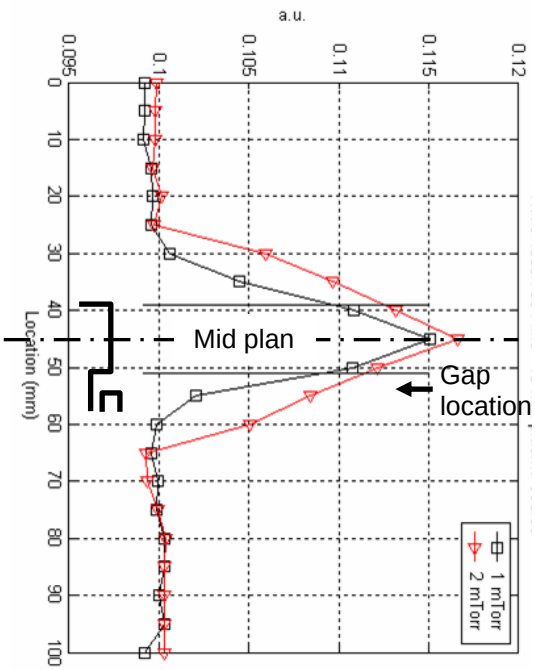

Figure 11. Variations of the ratio $I_\lambda(7504)/ I_\lambda(4609)$ emission lines along the magnet axis at two different pressures (1 mTorr and 2 mTorr in pure argon).

Microwave propagation modeling indicated that electric field intensity is higher in the gap vicinity than in the mid-plan of the magnet.
However, electrons trajectories simulations demonstrated that electrons energy gain is easier in the mid plan of the magnet while they are more often in this zone than in the gap vicinity. Another point must be stressed: in the mid-plan of the magnet relative orientation between electric field and magnetic field lines are nearly perpendicular. With such a configuration, ECR

coupling mechanism is more efficient in the mid-plan of the magnet where a weak HF field has been calculated than with a higher electric field and a weaker angular position between **E** and **B**. Experimental results obtained from OES located plasma production zone, fast electrons density area, in the mid plan of the magnet. This result is in good accordance with electrons trajectories simulation and microwave propagation modeling.

Further work will take into account these preliminary results to promote the ECR coupling in the existing region (mid-plan of the magnet) but also near the gap where electric field intensity is the higher.

8. References

[1] A. Lacoste, T. Lagarde, S. Béchu, Y. Arnal, J. Pelletier, *Multi-dipolar plasmas for uniform processing : physics, design and performance*, Plasma Sources Science Technol. 11, 407-412 (2002).

[2] D. D. Daineka, P. Bulkin, G. Girard, J.-E. Bourée, B. Drévillon, *High density plasma enhanced chemical vapour deposition of optical thin films*, (2004) Eur. Phys. J. Appl. Phys. 26 (3)

[3] T. V. Tran, thèse de 3° Cycle, Université Joseph Fourier – Grenoble (2006)

[4] G. Girard, S. Béchu, N. Caillault, L. Carbone, D. Fruchart, Bulk and thin films of magnetic shape memory Ni-Mn-Ga alloys deposited by multi-dipolar plasma assisted sputtering, soumis à Materiala

[5] L. Latrasse, N. Sadeghi, A. Lacoste, A. Bès, J. Pelletier, *Laser absorption and electric probe diagnostics for characterization of high density matrix microwave argon plasmas* , J. Phys. D : Appl. Phys. (soumis)

[6] Gaudin C., Rouille C., Serebrennikov K., Buzzi J. M., Bacal M., Lamoureux M., Charles P. ; *Source compacte de rayons X basée sur la résonance cyclotronique électronique (Compact X-ray source based on ECR)* ; Journal de physique. IV (J. phys., IV), ISSN 1155-4339 (1991).

[7] http://www.szxulong.com/Sm2Co17-new-en.htm

[8] J. Pelletier, 1995, *High density plasma sources: design, physics and performance*, ed. by O. Popov, Park Ridge, New Jersey (Noyes Publications), pp. 380-425